Enhanced Effects of Novel Oridonin Analog CYD0682 for Hepatic Fibrosis

Fredrick J. Bohanon, MD[a], **Xiaofu Wang, BS**[a], **Brittany M. Graham, BS**[a], **Chunyong Ding, PhD**[b], **Ye Ding, PhD**[b], **Cristiana Rastellini, MD**[a], **Jia Zhou, PhD**[b,*], and **Ravi S. Radhakrishnan, MD**[a,c,*]

[a]Department of Surgery, University of Texas Medical Branch, 301 University Blvd., Galveston, TX, 77555, USA

[b]Chemical Biology Program, Department of Pharmacology and Toxicology, University of Texas Medical Branch, 301 University Blvd., Galveston, TX, 77555, USA

[c] Department of Pediatrics, University of Texas Medical Branch, 301 University Blvd., Galveston, TX, 77555, USA

Abstract

Activated hepatic stellate cells (HSC) are responsible for excess extracellular matrix (ECM) protein deposition in liver fibrosis. Previously, our group reported that the natural compound oridonin induces apoptosis, inhibits cell proliferation, and down-regulates ECM proteins in activated HSC. In this study, the anti-fibrogenic effects of oridonin derivative CYD0682 on the activated human LX-2 and rat HSC-T6 stellate cell lines were investigated.

Methods—Cell proliferation was measured by Alamar Blue assay. Apoptosis was detected by Cell Death ELISA and staining of Yo-Pro-1 and propidium iodide. Cell cycle was determined by flow cytometry. Immunoblot and Immunofluorescence staining were performed for cellular protein expression.

*Send correspondence to: Ravi S. Radhakrishnan, Department of Surgery, The University of Texas Medical Branch, 301 University Boulevard, Galveston, Texas 77555-0353, Telephone: (409) 772-5666, FAX: (409) 772-4253, rsradhak@utmb.edu**Co-corresponding author:** Jia Zhou, Chemical Biology Program, Department of Pharmacology and Toxicology, University of Texas Medical Branch, Galveston, Texas 77555-0353, United States, Tel: (409) 772-9748; Fax: (409) 772-9648, jizhou@utmb.edu.

Results—CYD0682 treatment significantly inhibited LX-2 cells proliferation in a dose- and time-dependent manner with an IC_{50} value of 0.49 μM for 48 hours, ˜10–fold greater potency than oridonin. Similar results were observed in HSC-T6 cells. In contrast, 2.5 μM of CYD0682 treatment had no significant effects on proliferation of the human hepatocyte cell line C3A. CYD0682 treatment induced LX-2 cell apoptosis and S-phase cell cycle arrest, and was associated with activation of p53, p21, and cleaved-caspase-3. The myofibroblast marker protein α-smooth muscle actin and major ECM proteins type I collagen and fibronectin were markedly suppressed in a time- and dose-dependent fashion by CYD0682. Furthermore, pre-treatment with CYD0682 blocked TGFβ-induced type I collagen and fibronectin production.

Conclusion—In comparison with oridonin, its novel derivative CYD0682 may act as a more potent anti-hepatic fibrosis agent.

1. Introduction

Hepatic fibrosis is a final common pathway of both acute and chronic diseases that if left untreated may lead to cirrhosis [1-3]. In 2010, there were 31 million disability-adjusted life years lost and 2% of all deaths were due to liver cirrhosis [4]. Reversal of hepatic fibrosis and removal of the etiological agent may prevent this loss in quality and duration of life. Hepatic stellate cells (HSC) or previously known as Ito cells are a resident cell of the hepatic parenchyma and act as the major Vitamin A-storing cell [5]. In the quiescent state, the HSC regulates extracellular matrix (ECM) homeostasis, vasoregulation, and metabolic homeostasis [6].

Hepatic stellate cells (HSC) are the principal effector cells of the fibrogenic process [1, 3, 7-9]. Following liver injury, the HSC is activated, which is characterized by increased production of α-smooth muscle actin (α-SMA), loss of vitamin A stores, rapid proliferation, and production of extracellular matrix (ECM) proteins. A variety of stimuli were involved in HSC activation such as transforming growth factor β (TGF-β), lipopolysaccharide (LPS)/ toll-like receptors, tissue hypoxia, platelet-derived growth factors (PDGF), nicotinamide adenine dinucleotide phosphate-oxidase (NADPH), and the renin-angiotensin system [10, 11]. The deposition of ECM proteins and the phenotypic change of the HSC to a myofibroblast-like cell lead to fibrous tissue band formation that may lead to cirrhosis and liver failure [8].

Deactivation of HSC is a possible strategy for the treatment of hepatic fibrosis [10, 12]. Oridonin is an extract isolated from the plant *Rabdosia rubescens*, and has been studied extensively for its potent anti-inflammatory and anticancer effects [13-17]. Recently, our team reported on the antifibrotic effects of oridonin [18]. Oridonin inhibited HSC proliferation, induced cell cycle arrest, promoted apoptosis, and suppressed endogenous and transforming growth factor-β (TGF-β) induced ECM protein production [18]. However, in many cases, the potency of oridonin is relatively moderate. Therefore, it is imperative to develop novel derivatives of oridonin via structural modifications to enhance the potency. Zhou et al. developed several oridonin analogs and have demonstrated their anticancer effects to be more potent than oridonin [14, 19-21]. We hypothesize that the oridonin analog

CYD0682 will have similar anti-fibrogenic activity on activated hepatic stellate cells and be more potent than the parent compound.

2. Methods

2.1. Reagents

All cell culture mediums and trypsin were purchased from Life Technology Corp. (Carlsbad, CA). Oridonin was purchased from Sigma-Aldrich Co. LLC. (St. Louis, MO). Transforming growth factor β1 (TGF-β) was purchased from R&D Systems Inc. (Minneapolis, MN). Propidium iodide was purchased from MP Biomedicals, LLC (Solon, OH). HOESCHT 33342 (Cat#83218) was purchased from AnaSpec Inc.(Fremont, CA). CYD0682 is a novel analogue of 1-ene designed from oridonin by removal of 1-hydroxyl group and introduction of a double bond in the A-ring (Figure 1). CYD0682 was synthesized following our previously reported protocols [14].

2.2. Cell culture and treatment

The human immortalized HSC line LX-2 and rat immortalized HSC line HSC-T6 as well as the human hepatocyte cell lines C3A were purchased from American Type Cell Culture (ATCC, Manassas, VA) and cultured and cultured as described previously [18]. All experiments were performed on cells within 6 weeks of culture from liquid nitrogen. CYD0682 was dissolved in dimethyl sulfoxide (DMSO) at a 1:1000 dilution for cell treatments. DMSO (0.1%) was used for negative control.

2.3. Western immunoblotting

Whole cell extracts were prepared as previously described [18]. Antibody against α-smooth muscle actin (α-SMA) (Cat#5228) was purchased from Sigma-Aldrich Co. LLC. (St. Louis, MO). Anti-Collagen Type I polyclonal antibody (600-401-103) was purchased from Rockland Immunochemicals Inc. (Gilbertsville, PA). Antibodies against Fibronectin (sc-6952) were purchased from Santa Cruz Biotechnology Inc. (Santa Cruz, CA). GAPDH antibody (10R-G109A) was purchased from Fitzgerald Industries (Concord, MA). Anti-p21 (Cat#556431) was purchased from BD Biosciences (San Jose, CA). Anti-p53 (Cat#2527), phospho-p53 (Cat#9286), and phospho-Smad2/3 (Cat#8828) were purchased from Cell Signaling Technology Inc. (Danvers, MA). Apoptosis Western Blot Cocktail (ab136812) was purchased from Abcam (Cambridge, MA).

2.4. Detection of apoptosis

Cell Death Detection was carried out as previously described [18]. Apoptosis was determined using a Cell Death Detection ELISA Kit (product # 11 774 425 001, Roche Diagnostics Corp. Indianapolis, IN) following manufacturer's protocol. Assay was performed in duplicate and repeated twice. For the detection of apoptosis by Yo-Pro-1, we followed our previously described method [18]. Yo-Pro-1 uptake was determined by Nikon Eclipse Ti confocal microscope at 20X magnification (Nikon Instruments Inc. Melville, NY). For the detection of apoptosis by propidium iodide (PI) cells PI uptake was determined by Nikon Eclipse Ti confocal microscope at 20X magnification (Nikon Instruments Inc. Melville, NY) as previously described [18].

2.5. Immunofluorescence staining

Immunofluorescence staining was carried out as previously described [18]. After indicated treatments and staining, the cells were visualized by Nikon Eclipse Ti confocal microscope at 20X magnification (Nikon Instruments Inc. Melville, NY).

2.6. AlamarBlue/cell viability assay

Cell viability was assessed by AlamarBlue assay (Cat#Dal1025, Life Technologies, Grand Island, NY) following manufacturer's instructions. Fluorescence intensity was monitored using a SpectraMax M2 microplate reader (Molecular Devices, LLC, Sunnyvale, CA) with excitation and emission wavelengths set at 540 and 590 nm, respectively. Assay was performed in triplicate and repeated at least three times.

2.7. Cell cycle analysis by flow cytometry

Nuclear DNA content was measured by using PI staining and fluorescence-activated cell sorter analysis as previously described [18]. PI-stained nuclei were stored at 4°C at least 3 hours before fluorescence-activated cell sorter analysis using BD FACSCanto II flow cytometer (Becton, Dickinson and Company, Franklin Lakes, NJ) at the University of Texas Medical Branch Flow Cytometry and Cell Sorting Core Facility. ModFit LT for Win32 software was used for data analysis (Verity Software House, Inc., Topsham, ME).

2.8. Statistical analysis

Statistical analysis was performed using GraphPad Prism 5.0 (GraphPad Software Inc. La Jolla, CA).Data presented as mean ± standard error of the mean (SEM), with significance defined as $p < 0.05$.

3. Results

3.1. Inhibitory effects of CYD0682 on HSC proliferation is more potent than oridonin

The structure of CYD0682 as compared to the parent compound, oridonin, is shown in Figure 1. CYD0682 is a novel analogue of 1-ene designed from oridonin by removal of 1-hydroxyl group and introduction of a double bond in the A-ring. HSC proliferation is a hallmark of HSC activation and indicates the transformation from a quiescent to a myofibroblast phenotype [3]. To assess the antiproliferative effects of CYD0682 in comparison with oridonin, we treated human LX-2 cells for 48 hours at indicated concentrations and used Alamar Blue assay to determine cell viability. Dose response curves were calculated using GraphPad Prism 5.0 software (GraphPad Software, Inc., La Jolla, CA). Figure 2a demonstrates a significant increase in potency of CYD0682 compared to oridonin (IC_{50} 0.49 μM vs 7.33 μM, respectively; P<0.0001). CYD0682 further inhibits LX-2 proliferation in a time-dependent manner, following treatment for 24, 48, or 72 hours there was a 21.93% ± 2.35, 74.61% ± 0.85, and 70.03% ± 6.40 inhibition, respectively. Next, we determined the effects of CYD0682 on rat HSC-T6 cell line. Figure 2c illustrates similar findings to LX-2 cells with potent inhibition of growth at forty-eight hours with an IC_{50} calculated as 0.59 μM. Additionally, we measured the potency of CYD0682 on

hepatocytes (C3A cells) and obtained a significant reduction in potency with an IC_{50} of 3.28 μM (Figure 2d).

3.2. CYD0682 induces S-phase cell cycle arrest and inhibits HSC activation

The effects of CYD0682 on LX-2 cell cycle progression were assessed using flow cytometry. Since the majority of cells were in G0-G1 phase under resting conditions, the cells were not synchronized prior to flow cytometry. CYD0682 treatment for 24 hours results in a significant increase in S-phase cell cycle arrest compared to the control, 44.56% ± 2.56 vs. 30.20% ± 1.00, P = 0.0065 (Figure 3a). Next, cell cycle regulatory proteins were examined using Western blot following CYD0682 treatment for indicated time points. Figure 3b illustrates an increase in p21 expression levels with a 60% increase at 24 hours. Activated p53 (p-p53) expression levels were increased by 52% and 70% at 12 and 24 hours, respectively. α-SMA, a marker of HSC activation, was significantly reduced after CYD0682 (0.75 μM) treatment (Figure 3d, e) [8].

3.3. CYD0682 induces LX-2 cell apoptosis

The role of apoptosis in decreased LX-2 cell viability was explored. First, the Cell Death Detection ELISA, an assay that measures histone-associated DNA fragments which are markers of apoptosis, was used [22]. There was a significant induction of apoptosis following CYD0682 treatment after 24 hours. Next, Yo-Pro-1 and propidium iodide (PI) staining were used to determine if these effects were due to early or late apoptosis. Hoechst 33342 stains double-stranded DNA with an intact plasma membrane as a control, Yo-Pro-1 stains DNA in cells with a disrupted plasma membrane and is used as an early marker of apoptosis, whereas PI is a marker of late apoptosis [23, 24]. CYD0682 induced both early and late apoptosis in LX-2 cells (Figure 4b).

Finally, the involvement of the caspase cascade in CYD0682 induced apoptosis was examined. The ratio of cleaved-caspase 3 to procaspase 3 protein levels was elevated following CYD0682 treatment, suggesting that apoptosis occurred through a caspase-3 dependent pathway (Figure 4c).

3.4. CYD0682 downregulates endogenous ECM proteins in LX-2 cells

HSC activation results in an overexpression of ECM proteins, including type I collagen and fibronectin [25]. CYD0682 treatment significantly decreased the expression of type I collagen and Fibronectin. As early as 12 hours post treatment, type I collagen levels are significantly reduced as compared to the control (12 hours; 30% ± 1 p < 0.001. 24 hours; 24% ± 5 p < 0.05. 48 hours; 51% ± 10 p < 0.05. 72 Hours; 44% ± 10 p < 0.05). Fibronectin levels initially increase (12 hours; 45% ± 7 p < 0.05. 24 hours; 31% ± 6 p < 0.05.) then decline significantly at 72 hours (43% ± 7 p < 0.05) (Figure 5a). CYD0682 reduces type I collagen levels in a dose-dependent manner (Figure 5b). Immunofluorescence staining of type I collagen was performed on LX-2 cells following CYD0682 treatment. CYD0682 treatment results in a marked reduction in type I collagen (Figure 5c).

3.5. CYD0682 attenuates TGF-β-induced ECM production in LX-2 cells

TGF-β is one of the most potent stimulators of HSC [26, 27]. CYD0682 pretreatment for 24 hours followed by TGF-β stimulation for 24 hours resulted in a near complete inhibition of fibronectin and type I collagen (Figure 6a). CYD0682 had no significant effect on TGF-β – induced pSmad 2/3 protein levels (Figure 6b). Previously, our group demonstrated that oridonin resulted in a significant reduction in TGF-β-induced p-Smad 2/3 nuclear translocation and DNA binding [18]. Interestingly, CYD0682 did not significantly influence TGF-β-induced p-Smad 2/3 nuclear translocation or DNA binding (data not shown). Additionally, increasing concentrations of TGF-β (5 and 10 ng/mL) had similar expression of total Smad and p-Smad 2/3 (data not shown). Further, CYD0682 pretreatment or simultaneous treatment with 5 or 10 ng/mL TGF-β had the same effect as Figures 6 a, b, and c (data not shown).

4. Discussion

In this study, we investigated CYD0682, the potentially more potent anti-fibrogenic properties of the 1-ene analog of oridonin, compared to its parent compound. Natural compounds have played a significant role in human disease with over 150 common drugs in use today that were derived from natural products [28]. Natural products may have some issues including limited potency, efficacy and drug like properties that need to be optimized for further drug development. Some natural compounds may have limited availability from natural resources and have very complex structures that make synthesis and production costly and inefficient [29]. Oridonin is a naturally rich and readily available compound that has been extensively studied in the cancer and inflammation literature [15, 17, 30, 31]. Further, oridonin has been previously shown to inhibit HSC proliferation with a moderate potency, cause S-phase arrest, increase HSC apoptosis, attenuate endogenous α-SMA and ECM production and block TGF-β signaling [18]. The oridonin structure has several hydroxyl groups thus making it too polar with limited bioavailability.[16, 32] CYD0682 is a novel analog of oridonin newly designed by removal of 1-hydroxyl group on A-ring to improve lipophilicity thus improving the cell permeability and potency.[14]

CYD0682 has been shown to inhibit HSC proliferation with enhanced potency in both a time- and dose-dependent fashion. CYD0682 exhibits a 15-fold increase in IC_{50} value in HSC cells with minimal effect on C3A cell proliferation and viability as compared to oridonin. We chose C3A cells because they are a clonal derivative of the widely used human hepatocellular carcinoma HepG2 cell line and known for its better-differentiated hepatocyte phenotype.[33] Further, CYD0682 induced a significant increase in S-phase cell cycle arrest leading to deactivation of the HSC. CYD0682 significantly induced both early and late apoptosis in LX-2 cells. Finally, CYD0682 administration resulted in the attenuation of endogenous ECM production and inhibition of TGF-β-induced ECM production at a significantly lower concentration than oridonin [18].

HSC proliferation is a key step in the hepatic response to injury. Increased proliferation allows for a significant surge in ECM, cytokine, growth factor and α-SMA production [34]. CYD0682 demonstrated a potent ability to inhibit HSC proliferation and cell viability in both human and rat cell lines at much lower concentrations than the parent compound

oridonin. This was associated with an S-phase arrest and induction of apoptosis. G1/S checkpoint serves a major site of DNA repair regulation and is characterized by an increase in phosphorylated-p53 which causes an increase in p21 protein production [35]. Here, we show that CYD0682 treatment results in protein accumulation of phosphorylated-p53 and p21, which is often seen with S-phase cycle arrest, and may lead to cell death via apoptosis [35]. Apoptosis of HSC following CYD0682 treatment appears to be p53 dependent. Phosphorylated p53 may induce apoptosis via caspase-3 [36]. CYD0682 treatment increased expression of cleaved-caspase-3, suggesting a possible mechanism of apoptosis. This finding is different than the possible caspase-3 independent apoptosis pathway following oridonin treatment suggested previously [18].

Liver fibrosis is characterized by excessive accumulation of ECM proteins. A reduction in ECM protein production is a promising means of slowing or reversing the scar forming process [37]. CYD0682 treatment resulted in a significant reduction of endogenous and TGF-β-induced type I collagen and fibronectin production, achieving similar results to oridonin at a 10-fold less concentration. These findings may make CYD0682 a promising anti-fibrogenic agent. Type I collagen protein levels were significantly reduced in both a time- and dose-dependent fashion. Interestingly, fibronectin levels were initially elevated and later significantly reduced. This finding was also seen following oridonin treatment and the mechanism for this needs further elucidation [18]. TGF-β is one of the most potent stimulators of hepatic fibrosis [26]. Following TGF-β stimulation, the TGF-β receptor complex is activated and begins a series of protein interactions that most commonly activate Smad 2 and Smad 3. Smad 2 and 3 dimerize and translocate to the nucleus with Smad 4. Once in the nucleus, the complex activates transcription factors resulting in increased expression of ECM proteins most notably type I collagen and fibronectin [38]. Oridonin inhibited this signaling pathway, but CYD0682 appears to work through a Smad independent pathway. There have been recent reports of Smad independent TGF-β signaling in many models [39, 40]. These findings warrant deeper studies to determine the exact function of CYD0682.

This is an *in vitro* study of hepatic fibrosis using activated hepatic stellate cells. Further studies are imperative to identify and validate possible direct cellular targets of the drug candidate and translate to clinical use [41]. As the initial step of the normal sequence for drug development, the reported finding highlights the possible modes of action for CYD0682 in activated HSC.

5. Conclusion

In activated human and rat hepatic stellate cells, CYD0682 has demonstrated a significant ability to attenuate hepatic fibrogenesis *in vitro*. Further, CYD0682 is significantly more potent than its parent compound, oridonin. CYD0682 may have a great potential to act as a promising anti-fibrogenic agent for the treatment of hepatic fibrosis.

Acknowledgements

References

1. Hautekeete ML, Geerts A. The hepatic stellate (Ito) cell: its role in human liver disease. Virchows Arch. 1997; 430:195–207. [PubMed: 9099976]

2. Lee UE, Friedman SL. Mechanisms of hepatic fibrogenesis. Best Pract Res Clin Gastroenterol. 2011; 25:195–206. [PubMed: 21497738]

3. Puche JE, Saiman Y, Friedman SL. Hepatic stellate cells and liver fibrosis. Compr Physiol. 2013; 3:1473–1492. [PubMed: 24265236]

4. Novo E, Cannito S, Paternostro C, Bocca C, Miglietta A, et al. Cellular and molecular mechanisms in liver fibrogenesis. Arch Biochem Biophys. 2014; 548:20–37. [PubMed: 24631571]

5. Duval F, Moreno-Cuevas JE, Gonzalez-Garza MT, Rodriguez-Montalvo C, Cruz-Vega DE. Liver fibrosis and protection mechanisms action of medicinal plants targeting apoptosis of hepatocytes and hepatic stellate cells. Adv Pharmacol Sci. 2014; 2014:373295. [PubMed: 25505905]

6. Lee YA, Wallace MC, Friedman SL. Pathobiology of liver fibrosis: a translational success story. Gut. 2015; 64:830–841. [PubMed: 25681399]

6. Alter G, Heckerman D, Schneidewind A, Fadda L, Kadie CM, Carlson JM, Oniangue-Ndza C, Martin M, Li B, Khakoo SI, Carrington M, Allen TM, Altfeld M. HIV-1 adaptation to NK-cell-mediated immune pressure. Nature. 2011; 476:96–100. [PubMed: 21814282]

8. Li JT, Liao ZX, Ping J, Xu D, Wang H. Molecular mechanism of hepatic stellate cell activation and antifibrotic therapeutic strategies. J Gastroenterol. 2008; 43:419–428. [PubMed: 18600385]

9. Winau F, Hegasy G, Weiskirchen R, Weber S, Cassan C, et al. Ito cells are liver-resident antigen-presenting cells for activating T cell responses. Immunity. 2007; 26:117–129. [PubMed: 17239632]

10. Lemoinne S, Cadoret A, El Mourabit H, Thabut D, Housset C. Origins and functions of liver myofibroblasts. Biochim Biophys Acta. 2013; 1832:948–954. [PubMed: 23470555]

11. Tsukamoto H, Zhu NL, Wang J, Asahina K, Machida K. Morphogens and hepatic stellate cell fate regulation in chronic liver disease. J Gastroenterol Hepatol. 2012; 27(Suppl 2):94–98. [PubMed: 22320925]

12. Schuppan D, Kim YO. Evolving therapies for liver fibrosis. J Clin Invest. 2013; 123:1887–1901. [PubMed: 23635787]

13. Chen G, Wang K, Yang BY, Tang B, Chen JX, et al. Synergistic antitumor activity of oridonin and arsenic trioxide on hepatocellular carcinoma cells. Int J Oncol. 2012; 40:139–147. [PubMed: 21947421]

14. Ding C, Zhang Y, Chen H, Yang Z, Wild C, et al. Oridonin Ring A-Based Diverse Constructions of Enone Functionality: Identification of Novel Dienone Analogues Effective for Highly Aggressive Breast Cancer by Inducing Apoptosis. J Med Chem. 2013; 56:8814–8825. [PubMed: 24128046]

15. Liu Z, Ouyang L, Peng H, Zhang WZ. Oridonin: targeting programmed cell death pathways as an anti-tumour agent. Cell Prolif. 2012; 45:499–507. [PubMed: 23106297]

16. Xu W, Sun J, Zhang TT, Ma B, Cui SM, et al. Pharmacokinetic behaviors and oral bioavailability of oridonin in rat plasma. Acta Pharmacol Sin. 2006; 27:1642–1646. [PubMed: 17112421]

17. Zhou GB, Kang H, Wang L, Gao L, Liu P, et al. Oridonin, a diterpenoid extracted from medicinal herbs, targets AML1-ETO fusion protein and shows potent antitumor activity with low adverse effects on t(8;21) leukemia in vitro and in vivo. Blood. 2007; 109:3441–3450. [PubMed: 17197433]

18. Bohanon FJ, Wang X, Ding C, Ding Y, Radhakrishnan GL, et al. Oridonin inhibits hepatic stellate cell proliferation and fibrogenesis. J Surg Res. 2014; 190:55–63. [PubMed: 24742622]

19. Ding C, Zhang Y, Chen H, Yang Z, Wild C, et al. Novel nitrogen-enriched oridonin analogues with thiazole-fused A-ring: protecting group-free synthesis, enhanced anticancer profile, and improved aqueous solubility. J Med Chem. 2013; 56:5048–5058. [PubMed: 23746196]

20. Ding C, Zhang Y, Chen H, Wild C, Wang T, et al. Overcoming synthetic challenges of oridonin A-ring structural diversification: regio- and stereoselective installation of azides and 1,2,3-triazoles at the C-1, C-2, or C-3 position. Org Lett. 2013; 15:3718–3721. [PubMed: 23834026]

21. Ding C, Wang L, Chen H, Wild C, Ye N, et al. ent-Kaurane-based regio- and stereoselective inverse electron demand hetero-Diels-Alder reactions: synthesis of dihydropyran-fused diterpenoids. Org Biomol Chem. 2014; 12:8442–8452. [PubMed: 25225052]

22. Fielding AB, Dobreva I, McDonald PC, Foster LJ, Dedhar S. Integrin-linked kinase localizes to the centrosome and regulates mitotic spindle organization. J Cell Biol. 2008; 180:681–689. [PubMed: 18283114]

23. Fujisawa S, Romin Y, Barlas A, Petrovic LM, Turkekul M, et al. Evaluation of YO-PRO-1 as an early marker of apoptosis following radiofrequency ablation of colon cancer liver metastases. Cytotechnology. 2014; 66:259–273. [PubMed: 24065619]

24. Telford WG, King LE, Fraker PJ. Comparative evaluation of several DNA binding dyes in the detection of apoptosis-associated chromatin degradation by flow cytometry. Cytometry. 1992; 13:137–143. [PubMed: 1372208]

25. Kocabayoglu P, Friedman SL. Schol. Cellular basis of hepatic fibrosis and its role in inflammation and cancer. Front Biosci. 2013; 5:217–230.

26. Tahashi Y, Matsuzaki K, Date M, Yoshida K, Furukawa F, et al. Differential regulation of TGF-beta signal in hepatic stellate cells between acute and chronic rat liver injury. Hepatology. 2002; 35:49–61. [PubMed: 11786959]

27. Yoshida K, Matsuzaki K. Differential Regulation of TGF-β/Smad Signaling in Hepatic Stellate Cells between Acute and Chronic Liver Injuries. Front Physiol. 2012; 3:53. [PubMed: 22457652]

28. Lee KW, Thiyagarajan V, Sie HW, Cheng MF, Tsai MJ, et al. Synergistic effect of natural compounds on the fatty acid-induced autophagy of activated hepatic stellate cells. J Nutr Biochem. 2014; 25:903–913. [PubMed: 24857031]

29. Lam KS. New aspects of natural products in drug discovery. Trends Microbiol. 2007; 15:279–289. [PubMed: 17433686]

30. Tian W, Chen SY. Recent advances in the molecular basis of anti-neoplastic mechanisms of oridonin. Chin J Integr Med. 2013; 19:315–320. [PubMed: 23546635]

31. Xu Y, Xue Y, Wang Y, Feng D, Lin S, et al. Multiple-modulation effects of Oridonin on the production of proinflammatory cytokines and neurotrophic factors in LPS-activated microglia. Int Immunopharmacol. 2009; 9:360–365. [PubMed: 19185062]

32. Li, S.; Liu, Y.; Liu, T.; Zhao, L.; Zhao, J., et al. Int J Pharm. Vol. 2011. Elsevier B.V; Netherlands: 2011. Development and in-vivo assessment of the bioavailability of oridonin solid dispersions by the gas anti-solvent technique.; p. 172-177.

33. Kelly JH, Darlington GJ. Modulation of the liver specific phenotype in the human hepatoblastoma line Hep G2. In Vitro Cell Dev Biol. 1989; 25:217–222. [PubMed: 2466032]

34. March S, Graupera M, Rosa Sarrias M, Lozano F, Pizcueta P, et al. Identification and functional characterization of the hepatic stellate cell CD38 cell surface molecule. Am J Pathol. 2007; 170:176–187. [PubMed: 17200192]

35. Sancar A, Lindsey-Boltz LA, Ünsal-Kaçmaz K, Linn S. MOLECULAR MECHANISMS OF MAMMALIAN DNA REPAIR AND THE DNA DAMAGE CHECKPOINTS. Annual Review of Biochemistry. 2004; 73:39–85.

36. Cummings BS, Schnellmann RG. Cisplatin-Induced Renal Cell Apoptosis: Caspase 3-Dependent and -Independent Pathways. Journal of Pharmacology and Experimental Therapeutics. 2002; 302:8–17. [PubMed: 12065694]

37. Bataller R, xF, Brenner DA. Liver fibrosis. The Journal of Clinical Investigation. 2005; 115:209–218. [PubMed: 15690074]

38. Gressner AM, Weiskirchen R, Breitkopf K, Dooley S. Roles of TGF-beta in hepatic fibrosis. Front Biosci. 2002; 7:d793–807. [PubMed: 11897555]

39. Derynck R, Zhang YE. Smad-dependent and Smad-independent pathways in TGF-beta family signalling. Nature. 2003; 425:577–584. [PubMed: 14534577]

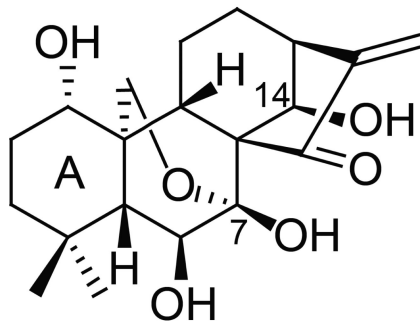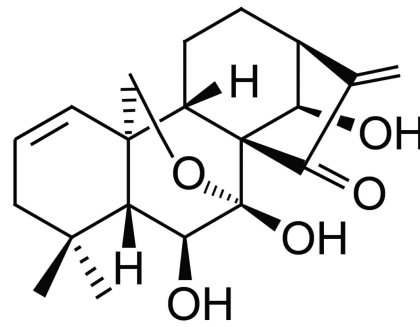40. Moustakas A, Heldin CH. Non-Smad TGF-beta signals. J Cell Sci. 2005; 118:3573–3584. [PubMed: 16105881]

41. Trautwein C, Friedman SL, Schuppan D, Pinzani M. Hepatic fibrosis: Concept to treatment. J Hepatol. 2015; 62:S15–s24. [PubMed: 25920084]
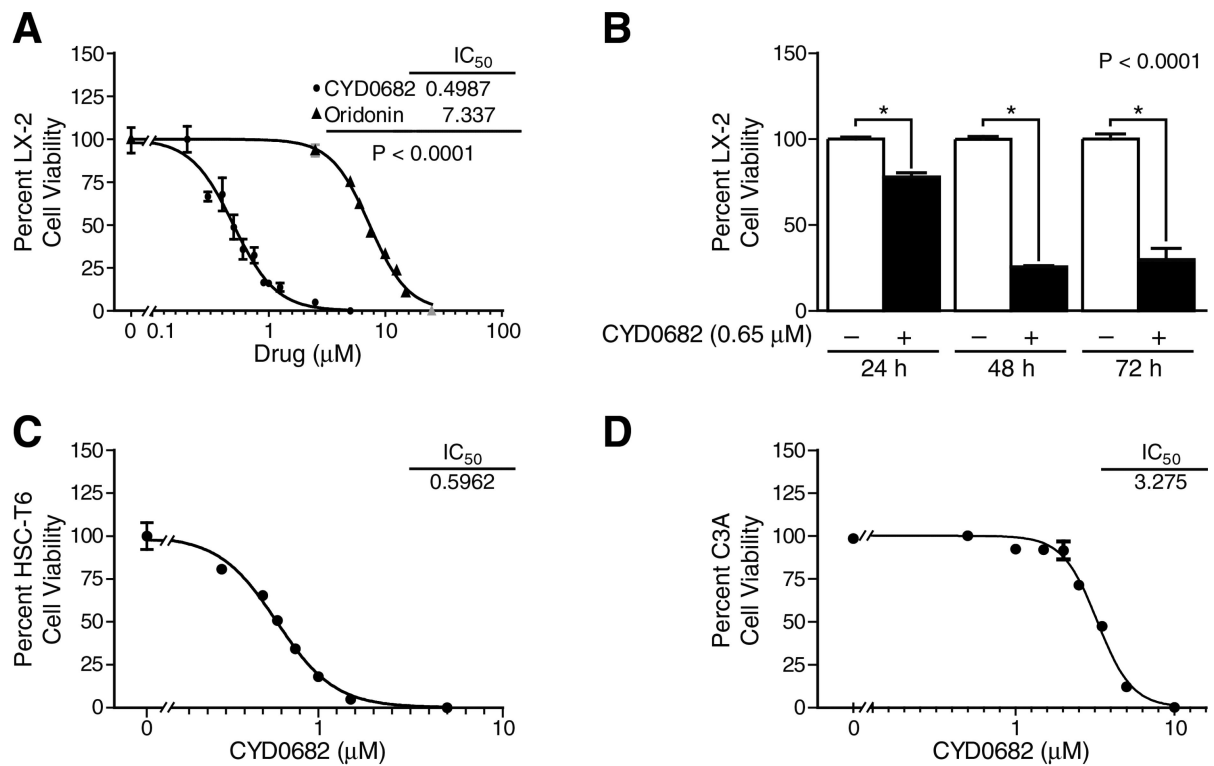
Oridonin

CYD0682

Figure 1.
Chemical structures of oridonin and its new analogue CYD0682.

Figure 2. CYD0682 more potently inhibits HSC proliferation than oridonin
LX-2 cells (A), HSC-T6 cells (C) and C3A hepatocytes (D) were treated with a series of concentrations of CYD0682 for 48 hours, and cell viability was determined using Alamar Blue assay. Dose response curves were calculated using GraphPad Prism 5.0. LX-2 cells were treated with 0.75 μM of CYD0682 for 24, 48, and 72 hours; cell viability was measured by Alamar Blue assay (B). P-values shown compared to vehicle (0.1% DMSO, 0 μM). The results are representative of at least three independent experiments.
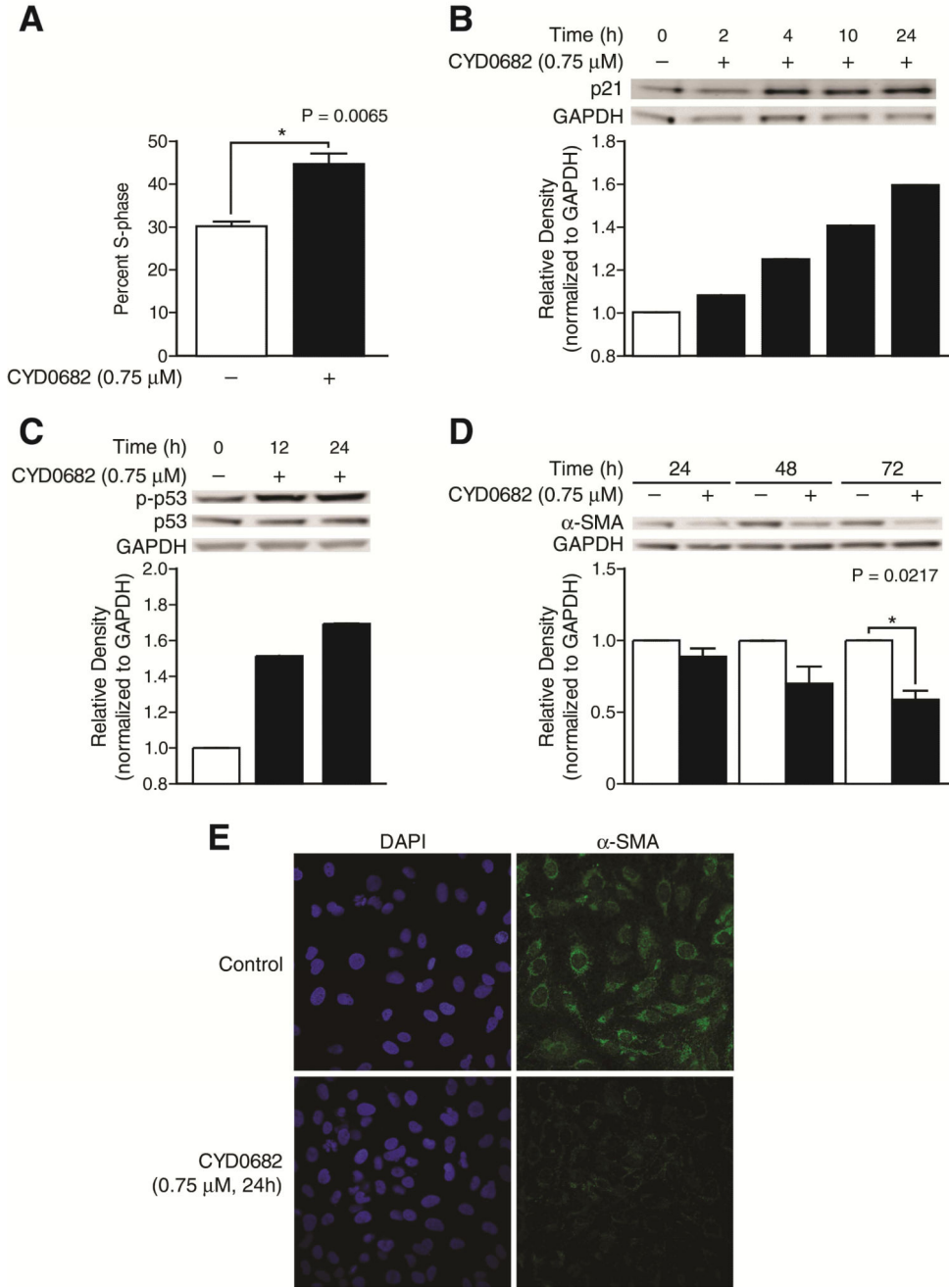
Figure 3. CYD0682 induces LX-2 cell cycle arrest

CYD0682 induces S-phase cell cycle arrest (A). LX-2 cells were treated with CYD0682 (0.75 μM) for 24 hours. Cells were stained with propidium iodide and analyzed by flow cytometry as described in Methods. (B) and (C) CYD0682 affects cell cycle regulatory proteins. LX-2 cells were treated with vehicle (0.1% DMSO) or CYD0682 (0.75 μM) for indicated time points. Whole cell lysates were analyzed by Western blot with antibodies for p53, p-p53, and p21. CYD0682 inhibits α-SMA expression (D). Whole cell lysates were analyzed by Western blot with antibodies for α-SMA. GAPDH was used as loading control.
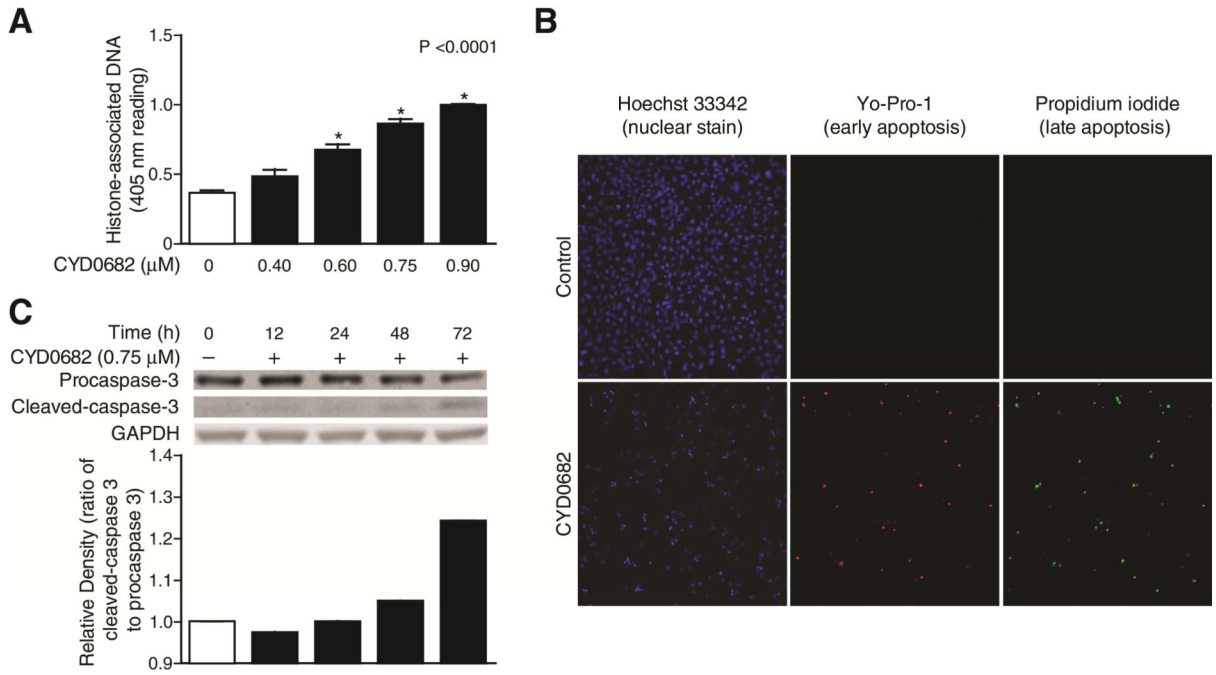
The experiments were repeated three times and representative data are shown. α-SMA immunofluorescence (green) is marked reduced following CYD0682 treatment (E). LX-2 cells were treated with CYD0682 (0.75 μM) for 24 hours and stained as described in Methods. DAPI staining was used as a control (blue).

Figure 4. CYD0682 promotes LX-2 cell apoptosis
Apoptosis by CYD0682 was evaluated by Cell Death detection ELISA (each conducted in triplicate) after CYD0682 treatment (at indicated concentrations) for 24 hours. CYD0682 treatment resulted in significant apoptosis (A). Early and late apoptosis were elevated following CYD0682 (0.75 μM) treatment for 24 hours (B). Hoechst 33342 is a nuclear stain used as a control. Yo-Pro-1 is a marker of early apoptosis and propidium iodide is a marker of late apoptosis. Whole cell lysates were analyzed by Western blot with antibodies for procaspase 3 and cleaved-caspase3 (C). LX-2 cells were treated at indicated time points with 0.75 μM of CYD0682. GAPDH was used as a loading control. The results are representative of at least three independent experiments.
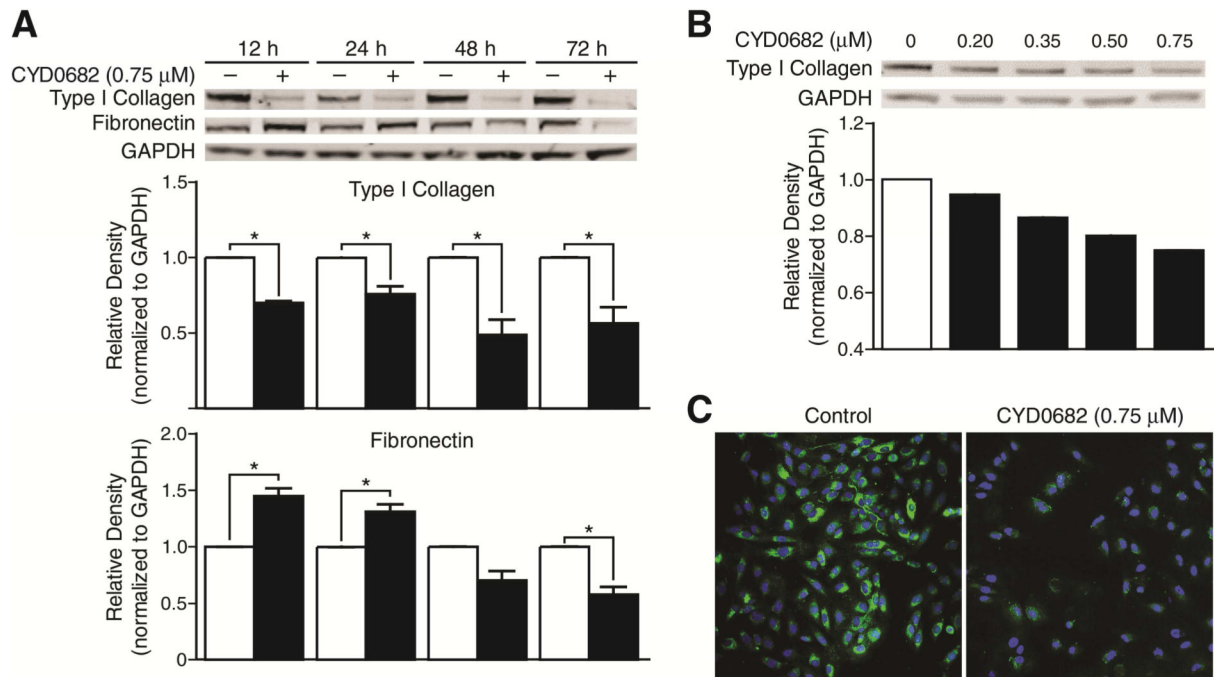
Figure 5. CYD0682 suppresses endogenous ECM protein expression

LX-2 cells were incubated with CYD0682 (0.75 μM) at time points as indicated. Whole cell lysates were analyzed by Western blot with antibodies for type I collagen and fibronectin (A). LX-2 cells were treated with CYD0682 at indicated doses for 24 hours (B). GAPDH was used as loading control. The results are representative of at least three independent experiments. LX-2 cells were treated for 24 hours with 0.75 μM of CYD0682 and stained for type I collagen (green) and DAPI nuclear stain (blue). The images were overlaid and demonstrate a drastic reduction in type I collagen staining (C).
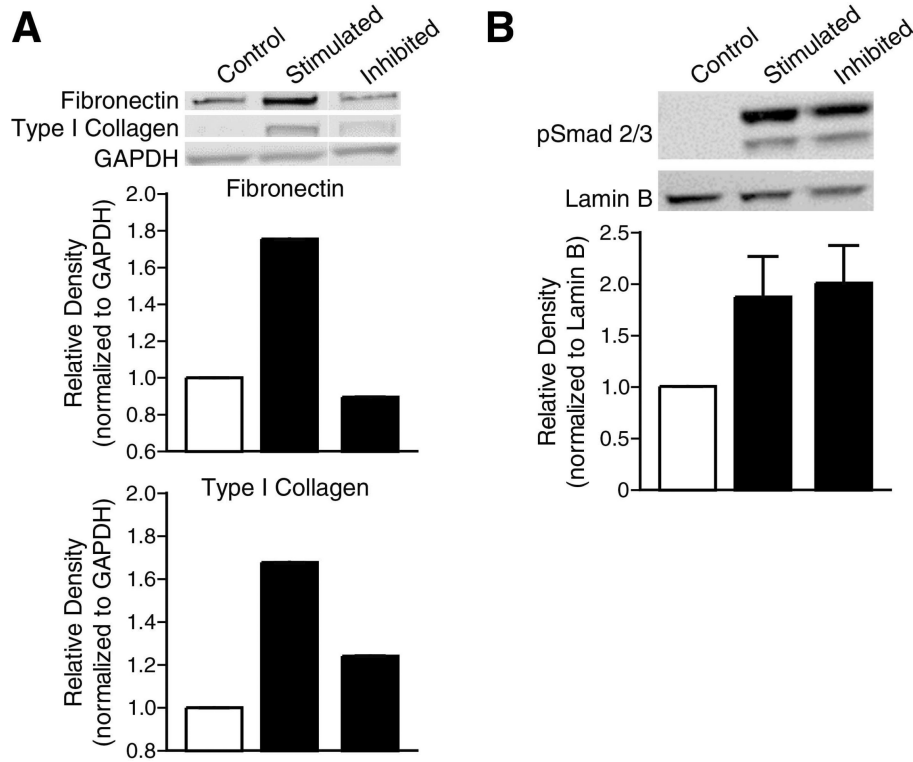
Figure 6. CYD0682 inhibits TGF-β induced pSmad activity and ECM production
LX-2 cells were preincubated with CYD0682 (0.75 μM) for 24 hours and then treated with TGF-β (2 ng/mL) for 24 hours, whole cell lysates were analyzed by Western blot with antibodies for fibronectin and type I collagen (A). GAPDH was used as loading control. Nuclear protein levels of phosphorylated-Smad2/3 were analyzed by Western blot (B). Lamin B was used as a loading control. The results are representative of at least three independent experiments.